Molecular dissociation in the presence of catalysts: interpreting bond breaking as a quantum dynamical phase transition

2015 J. Phys.: Condens. Matter 27 315501

(http://iopscience.iop.org/0953-8984/27/31/315501)

IOP Publishing Journal of Physics: Condensed Matter
J. Phys.: Condens. Matter **27** (2015) 315501 (7pp) doi:10.1088/0953-8984/27/31/315501

Molecular dissociation in the presence of catalysts: interpreting bond breaking as a quantum dynamical phase transition

A Ruderman[1,2], A D Dente[3], E Santos[1,2] and H M Pastawski[1]

[1] Instituto de Física Enrique Gaviola (CONICET), Facultad de Matemática, Astronomía y Física, Universidad Nacional de Córdoba, 5000 Córdoba, Argentina
[2] Institute of Theoretical Chemistry, Ulm University, D-89069 Ulm, Germany
[3] INVAP S.E., 8403, San Carlos de Bariloche, Río Negro, Argentina

E-mail: horacio@famaf.unc.edu.ar

Received 4 March 2015, revised 8 June 2015
Accepted for publication 24 June 2015
Published 20 July 2015

Abstract

In this work we show that molecular chemical bond formation and dissociation in the presence of the *d*-band of a metal catalyst can be described as a quantum dynamical phase transition (QDPT). This agrees with DFT calculations that predict sudden jumps in some observables as the molecule breaks. According to our model this phenomenon emerges because the catalyst provides for a non-Hermitian Hamiltonian. We show that when the molecule approaches the surface, as occurs in the Heyrovsky reaction of H_2, the bonding H_2 orbital has a smooth crossover into a bonding molecular orbital built with the closest H orbital and the surface metal *d*-states. The same occurs for the antibonding state. Meanwhile, two resonances appear within the continuous spectrum of the *d*-band, which are associated with bonding and antibonding orbitals between the furthest H atom and the *d*-states at the second metallic layer. These move toward the band center, where they collapse into a pure metallic resonance and an almost isolated H orbital. This phenomenon constitutes a striking example of the non-trivial physics enabled when one deals with non-Hermitian Hamiltonian beyond the usual wide band approximation.

Keywords: atoms, molecule, transition

(Some figures may appear in colour only in the online journal)

1. Introduction

When do two individual atoms become a molecule, or vice versa? This question is a fundamental one for chemistry as much as it is for physics. Certainly, it should involve a sort of discontinuity as in a phase transition. In this context, Anderson hinted in his well-known article 'More is different' [1][4] that a condition for a quantum phase transition is the presence of infinite degrees of freedom. Sometimes, these are provided by the environment [2].

A paradigmatic example of molecular formation and dissociation is the Heyrovsky reaction [3], one of the steps of the hydrogen evolution reaction at metallic electrodes; after the adsorption of a hydrogen atom at the surface, a second proton approaches and an electron is transferred from the metal. It is during this last step when the hydrogen molecule is formed and a discontinuity is hinted by DFT calculations as a jump in energy and spin polarization. This occurs at a critical distance of the farthest hydrogen [4].

In quantum mechanics, a phase transition is recognized as a non-analytic behaviour of an observable, typically the ground state energy, as a function of a control parameter. This

[4] [1] States explicitly: 'the essential idea is that in the so-called $N \to \infty$ limit of large systems (on our own, macroscopic scale) it is no only convenient but essential to realize that matter will undergo mathematically sharp, singular 'phase transitions' to states in which the microscopic symmetries, and even the microscopic equations of motion, are in a sense violated'.

phenomenon, absent in a few atom systems, is an emergent property of the thermodynamic limit, i.e. when N, the number of atoms or degrees of freedom, tends to infinity [5, 6]. Such a limit is a necessary condition for the Fermi Golden Rule (FGR). For concreteness, let us recall the case of an adatom introduced in the Anderson–Newns theory of adsorption [7, 8]. This is often invoked to describe molecular dissociation and electrocatalysis when an atom of energy E_B interacts with the surface of a metal described by N eigenenergies E_k [9]. In assessing the effect of the interactions $V_{B,k}$ through the second order perturbation theory, one assigns an infinitesimal imaginary part $-\mathrm{i}\eta$ to each of the N involved metal energies, $\Delta E_B = \sum_k |V_{B,k}|^2/(E_B - E_k + \mathrm{i}\eta)$. Then, η is made zero only after taking $N \to \infty$ [2]. Thus, the initial energy E_B acquires, besides the expected real shift Δ_0, an imaginary correction Γ_0. This describes a finite energy uncertainty or broadening associated with a decay rate $2\Gamma_0/\hbar$. A straightforward way to account for this decay is to introduce an effective non-Hermitian Hamiltonian where the adatom energy acquires an imaginary component, e.g. $E_B \to E_B + \Delta_0 - \mathrm{i}\Gamma_0$. Although this procedure dates back to Majorana [10], its deep physical implications only recently became evident. One of these is the possibility of a quantum dynamical phase transition (QDPT) [11].

Clear experimental evidence of such a dynamical transition was shown in NMR experiments in a $2(CH)_5Fe$ crystal. There, the nuclear spins of the rare ^{13}C-^{1}H dimers can perform Rabi oscillations. Beyond some critical crystal orientation, these spins are seen to abruptly decouple. This occurs when the interaction between the ^{1}H spin and the rest of the crystal becomes stronger than the ^{13}C-^{1}H one [11]. This QDPT can also be interpreted as a particular case of the superradiance phenomenon predicted by Dicke [12–16]. This discontinuity suggests that the atom-molecule transition observed both in nature and DFT calculations could also be a form of QDPT. Thus, the main objective of this work is to provide the essential conceptual ingredients that feed this idea.

As a preliminary notion of how a non-Hermitian Hamiltonian can provide a framework for non-analytical discontinuity, let us consider the simplest tight-binding model for a homonuclear diatomic molecule $A - B$ interacting with a metal. This model would display some of the concepts relevant for the main discussion with much simpler algebra. Let $\delta E_0 = 2V_{AB}$ be the usual bonding-antibonding splitting (figure 1(a)). In this case, atom B has a hypothetical interaction with a wide metallic sp-band of width W_{sp}. When $W_{sp} \gg \delta E_0$, $-\mathrm{i}\Gamma_0$ does not depend on the precise position of the atomic energies respective of the band center and the shift results, then $\Delta_0 \equiv 0$. This is the wide band approximation, where the weak tunnelling into the metal, $\Gamma_0/2 \ll W_{sp}$, is our free parameter that accounts for the interaction. This results in the effective non-Hermitian molecular Hamiltonian [10],

$$\mathbb{H}_{\text{eff.}} = \begin{bmatrix} E_A & -V_{AB} \\ -V_{AB} & E_B - \mathrm{i}\Gamma_0 \end{bmatrix}. \tag{1}$$

The eigenenergies of $\mathbb{H}_{\text{eff}}$ are now complex numbers. The difference between their real parts is the splitting between the bonding and antibonding molecular levels, $\delta E = \sqrt{[\delta E_0]^2 - \Gamma_0^2}$. This splitting is now weakened by the interaction with the substrate. Their corresponding imaginary parts $\Gamma_0/2$ are identical. However, $\delta E(\Gamma_0)$ has a non-analytic collapse when Γ_0 reaches the critical value $\Gamma_c = \delta E_0$. Beyond this Exceptional Point (EP) [17–20], the real parts of the eigenvalues become degenerate while the imaginary parts bifurcate. For $\Gamma_0 \gg \delta E_0$ values, one of the eigenvalues is associated with B and has an imaginary part Γ_0 that indicates that B remains strongly mixed with the substrate. The other eigenvalue is associated with A and has an uncertainty proportional to $|2V_{AB}|^2/\Gamma_0$. This indicates an almost isolated orbital [10]. The detailed analytical and numerical solution of the above model is discussed in great detail in the context of QDPT by Dente *et al* [21].

Although very appealing for its simplicity *this previous picture can not be directly applied to a typical metallic catalyst*, it is in a very different physical regime. The delocalized orbitals that constitute the wide sp-band does not have enough overlap with the molecule orbitals to afford a relevant role in the molecular dissociation. Thus, our attention should turn to the strong interaction of the molecule with the highly oriented orbitals of the d-band [22]. These orbitals have large overlap with the molecule orbitals and have long been recognized as responsible for catalysis [8]. However, in general, the d-band has a width W_d smaller than the molecular level splitting δE_0; see figure 1(b)). This prevents using the wide band approximation and the previous analysis. Thus, the sp-band has the width but not the interaction strength to provide a transition, and the the d-band has the interaction strength but not enough width to support the previous analysis. Consequently, we are back to the question of *which mechanism could lead to non-analyticity associated with bond breaking in presence of a d -band?*

In this article, we answer this question to solve our model exactly, i.e. beyond the wide band limit and the Fermi Golden Rule. This will allow us to show that an actual analytical discontinuity appears if one includes a description of the metallic d-band with enough detail. This requires choosing an appropriate combination between the molecular levels and the different metallic layers and solving them in a non-perturbative way. In our terms, while the molecule approaches to the surface, the farther A atom experiences a resonant through-bond coupling [23] with the second layer of the metal. This interaction, mediated by the B atom and the first surface layer, manifests as two resonances inside the d-band. The transition occurs when these resonances collapse at the center of the d-band, releasing the A atom. Meanwhile, the B atom hybridization with A is swapped into B-metal bonding.

2. A model for molecule dissociation

We consider the molecule Hamiltonian to be $\hat{H}_S = E_A|A\rangle\langle A| + E_B|B\rangle\langle B| - V_{AB}(|A\rangle\langle B| + |B\rangle\langle A|)$. The degeneracy of the atomic energies E_A and E_B is broken by the bonding interaction V_{AB}. According to the standard wisdom [9], the d_{z^2} (top) or combination of the d_{xz} and d_{yz} (for hollow sites) are the only d-orbitals with a finite overlap with the molecule. The orbital $|B\rangle$ interacts with the closest d-orbital combination,

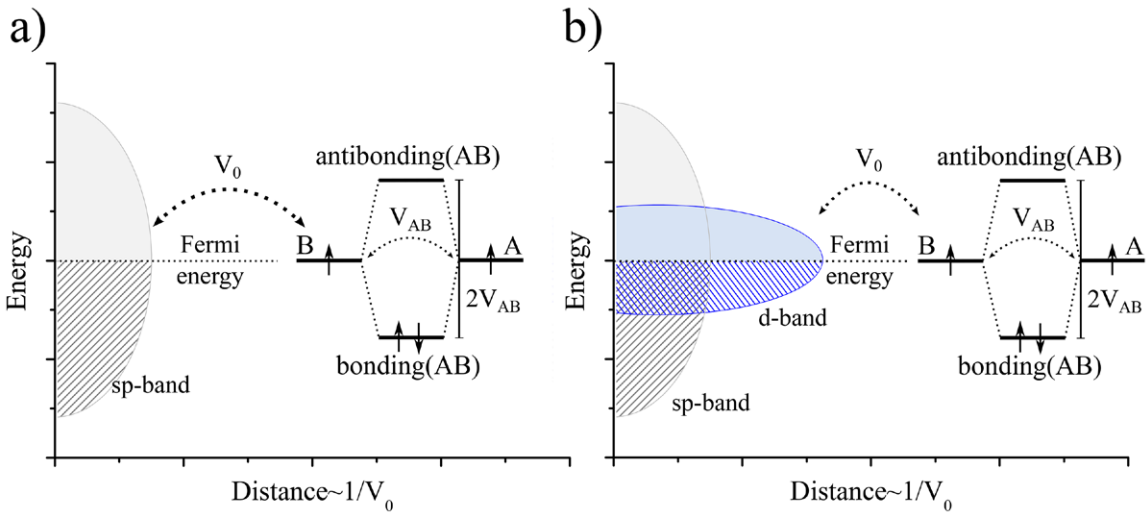

Figure 1. (a) Energy levels of an *sp*-band interacting with atomic orbital B through V_0. The molecular levels are also shown to support the validity of the wide band approximation. V_0 leads to the level broadening Γ_0. This case does not describe the catalysis process. (b) Energy levels of an *d*-band interacting with the atomic orbital B through V_0. The molecular levels are also shown to stress the fact that their splitting is further widened by the interaction V_0. This model is suitable for describing the catalysis.

for example $|1\rangle$, going along the connecting path through the binding energy V_0, $\hat{V}_{\rm SM} = -V_0(|B\rangle\langle 1| + |1\rangle\langle B|)$. The interaction energy V_0 is approximately an exponential function of the molecule-substrate distance. Therefore, the complete Hamiltonian becomes $\hat{H} = \hat{H}_{\rm S} + \hat{H}_{\rm M} + \hat{V}_{\rm SM}$. This can describe the Heyrovsky reaction, i.e. a H_2 molecule approaching perpendicularly to the metal surface.

Let us now focus on $\hat{H}_{\rm M}$, which describes the *d*-band. Since the pioneering work of Newns [8], it is usually assumed that a semi-elliptical shape is a good approximation for the Local Density of States (LDoS):

$$N_d(\varepsilon) = \frac{1}{\pi W_d}\sqrt{W_d^2 - 4\varepsilon^2} \times \Theta[W_d - 2\varepsilon] \times \Theta[2\varepsilon - W_d], \quad (2)$$

where $\Theta[x]$ is the Heaviside function. Indeed, the validity of this proposal for an actual metal can be visualized through the Lanczos transformation [24]. This is a unitary transformation that maps the actual $3D$ substrate into an equivalent $1D$ linear chain. Figure 2 represents this procedure for a $2D$ case. Starting from the $|1\rangle$ surface *d*-orbital, a sequence of 'collective orbitals' is built up mainly from the atomic orbitals at layers progressively distant from the original surface orbital. Regardless of the precise original Hamiltonian $\hat{H}_{\rm M}$, according to Lanczos the metal Hamiltonian $\hat{H}_{\rm M}^{\rm L}$ has identical 'site' energies $E_n \equiv E_d$ and only nearest neighbor V_n interactions that account for the coupling among the Lanczos collective states [24]. Their rapid convergence to $V_\infty \equiv V = W_d/4$ justifies the Newns proposal of a homogeneous linear chain to describe the actual metal. The kets $|n\rangle$ are the collective *d*-orbitals, now the nth site of the metallic chain. On the surface of the metal the coupling between layers is weaker than in the bulk, so we assume $|V_1| \lesssim |V_2| \lesssim |V|$ and we set $V_n \equiv V$ for $n \geqslant 3$.

$$\hat{H}_{\rm M}^{\rm L} = \sum_{n=1}^{\infty} E_n|n\rangle\langle n| + \sum_{n=1}^{\infty} -V_n(|n\rangle\langle n+1| + |n+1\rangle\langle n|). \quad (3)$$

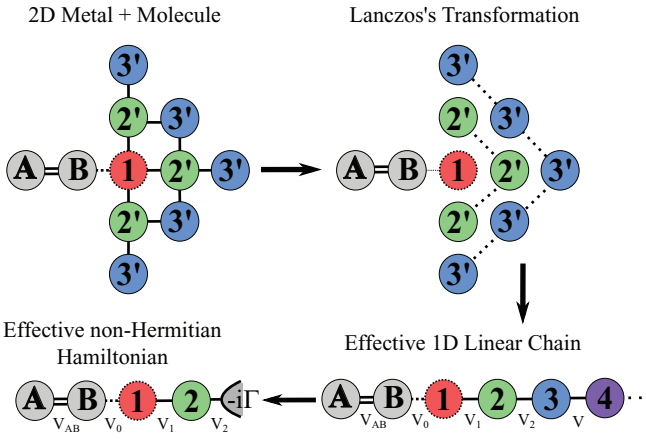

Figure 2. Effective non-Hermitian Hamiltonian: diatomic A–B molecule (in gray) in a configuration perpendicular to a $2D$ metal. The Lanczos unitary transformation combines orbitals at the same distance. The resulting tridiagonal Hamiltonian can be represented as a linear chain. A decimation procedure leads to a 4×4 non-Hermitian Hamiltonian. The same procedure can be applied to the $3D$ metal. Dot 1 represents a single atom for *top* interaction or a combination of them for *hollow*.

With the purpose of defining an optimal configuration for the molecular dissociation we base our model on the Anderson–Newns theory and set up the Fermi energy level at E_d, the center of the *d*-band, and thus $E_A = E_B = E_d$. Thus, the molecular bonding V_{AB} yields a symmetric splitting around the center of the band. Additionally, we set the coupling elements $V_1/V = 0.8$, $V_2/V = 0.9$, and $V_{AB}/V = 2.5$, which results in various fairly representative situations [25].

At this point it is necessary to list some of the main approximations implied by this model. First, the fixed value of V_{AB} neglects the variation of the distance between the atoms A and B. This does not affect our main results since the molecule breaking can be viewed as a competence among interactions. Second, as usual the atoms in the metal are considered fixed

in the whole problem. However, variations are minor in the Lanczos approach. Third, We assume a null coupling between the metal and A the furthest atom. A residual exponentially small interaction would be completely masked by the through-bond interaction.

3. Molecule dissociation as a spectral bifurcation

The solution of a linear chain model is better expressed in terms of the retarded Green's function matrix $\mathbb{G} = (\varepsilon\mathbb{I} - \mathbb{H})^{-1}$, whose divergences occur at the Hamiltonian eigenstates. For example, for the case of equation (1), in absence of a metal, we have $\Gamma_0 \equiv 0$ and:

$$G^{(S)}_{AA}(\varepsilon) = \frac{1}{\varepsilon - E_A - \Sigma_A(\varepsilon)}, \text{ where } \Sigma_A(\varepsilon) = \frac{|V_{AB}|^2}{\varepsilon - E_B}. \quad (4)$$

Clearly, E_A, the isolated A atom energy, is modified by the presence of B through the self-energy $\Sigma_A(\varepsilon)$, which here is a real function accounting for the bond and providing for the exact molecular bonding and antibonding eigenenergies. As discussed, one uses a regularization energy η, $\tilde{E}_k = E_k - \mathrm{i}\eta$ (for $k = A, B, n$) to facilitate the study of the spectral density. This also accounts for restricted charge dynamics whose physical origin can be traced back to small 'environmental interactions', a possible role played by the *sp*-band states [26]. When the molecule is coupled with the *d*-band, the retarded Green's function results [27]:

$$G_{AA}(\varepsilon) = \cfrac{1}{\varepsilon - \tilde{E}_A - \cfrac{|V_{AB}|^2}{\varepsilon - \tilde{E}_B - \cfrac{|V_0|^2}{\varepsilon - \tilde{E}_1 - \cfrac{|V_1|^2}{\varepsilon - \tilde{E}_2 - \cfrac{|V_2|^2}{|V|^2}\Sigma(\varepsilon)}}}}. \quad (5)$$

Here, $\Sigma(\varepsilon)$ is the self-energy correction describing the bulk of the metal *d*-band in the Lanczos representation:

$$\Sigma(\varepsilon) = \frac{|V|^2}{\varepsilon - \tilde{E}_d - \Sigma(\varepsilon)} = \Delta(\varepsilon) - \mathrm{i}\Gamma(\varepsilon) \quad (6)$$

from now on we set $E_d = 0$, and, thus, the solution of equation (6) results [28]:

$$\Sigma(\varepsilon) = \frac{\varepsilon + \mathrm{i}\eta}{2} - \mathrm{sgn}(\varepsilon) \cdot \left(\sqrt{\frac{r+x}{2}} + \mathrm{i} \cdot \mathrm{sgn}(y) \cdot \sqrt{\frac{r-x}{2}} \right), \quad (7)$$

with $x = \frac{\varepsilon^2 - \eta^2}{2} - V^2$, $y = \frac{\varepsilon\eta}{2}$ and $r = \sqrt{x^2 + y^2}$. For the effective site at the second layer we have:

$$G_{22}(\varepsilon) = \frac{1}{\varepsilon + \mathrm{i}\eta - \Sigma_{2L}(\varepsilon) - \frac{|V_2|^2}{|V|^2}\Sigma(\varepsilon)}, \quad (8)$$

with

$$\Sigma_{2L}(\varepsilon) = \cfrac{|V_1|^2}{\varepsilon + \mathrm{i}\eta - \cfrac{|V_0|^2}{\varepsilon + \mathrm{i}\eta - \frac{|V_{AB}|^2}{\varepsilon + \mathrm{i}\eta}}}, \quad (9)$$

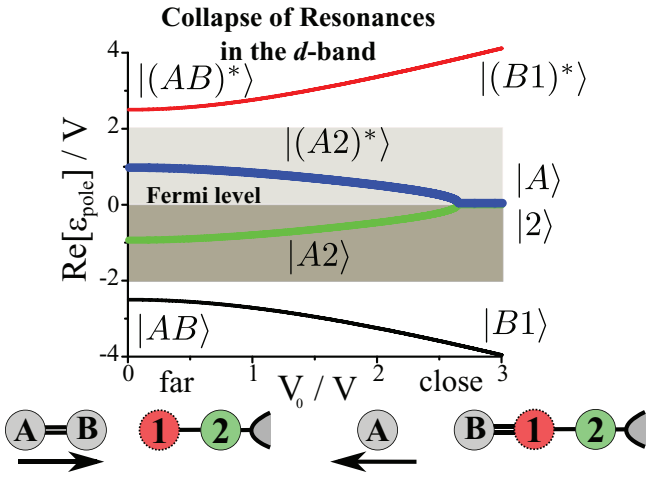

Figure 3. Collapse of resonances in the *d*-band. The real part of the poles is plotted versus the molecule–substrate interaction, V_0. Small V_0 values represent a far away molecule. For larger V_0's the molecule is close to the metal. The gray area represents the *d*-band, which goes from −2 V to 2 V. Outside the band the bonding molecular orbital $|AB\rangle$ smoothly becomes a bonding combination between the atom and the metal $|B1\rangle$ (black curve). The same occurs for the antibonding state $|(AB)^*\rangle$ that becomes $|(B1)^*\rangle$ (red curve). Poles within the d-band correspond to the bonding and antibonding resonances $|A2\rangle$ and $|(A2)^*\rangle$ (green and blue curves, respectively); after the transition they become an almost isolated $|A\rangle$ orbital and a $|2\rangle$ orbital strongly coupled to the metal.

and similar equations for the other sites. In all these cases the LDoS is obtained from the imaginary part of the Green's function: $N_i(\varepsilon) = -\frac{1}{\pi}\lim_{\eta\to 0} \mathrm{Im}[G_{ii}(\varepsilon)]$.

The imaginary part of the self-energy $\Sigma(\varepsilon)$ accounts for the quantum diffusion of the electrons into the metallic substrate. In a finite system $\Sigma(\varepsilon)$ would be a collection of divergences at discrete eigenenergies as $\Sigma_{2L}(\varepsilon)$. In contrast, the imaginary part, $\Gamma(\varepsilon)$, and the continuum spectrum are consequences of taking the thermodynamic limit of infinitely many sites in the chain. Within the *d*-band, the imaginary part survives the limit $\eta \to 0^+$, indicating that each atomic orbital merges into the metallic band [29]. However, the mere existence of $\Gamma \neq 0$ does not warrant the QDPT. In this narrow band model, a QDPT emerges as consequence of the specific non-linear dependence of Γ and Δ on ε, which accounts for the different metal layers. This is also responsible for the fully non-Markovian nature of our treatment [30]. The crucial distinction with respect to the introductory example is that the self-energies acquire a non-linear dependence on ε that contains all the wealth of the molecule–catalyst interaction.

Finding the corresponding energy spectrum involves a fourth-order polynomial on ε with complex coefficients. A simple procedure is to find the eight complex roots of $|1/G_{AA}(\varepsilon)|^2$. Half of them are non-physical because they are divergences for $|G_{AA}(\varepsilon)|^2$ but not for $G_{AA}(\varepsilon)$. Thus, we evaluate the poles numerically. Once we obtain the solutions, we choose the physical ones, i.e. those whose imaginary component is negative, i.e. poles of the retarded Green's function.

In figure 3 we show the real part of the Green's function poles. There, we observe two energies outside the *d*-band,

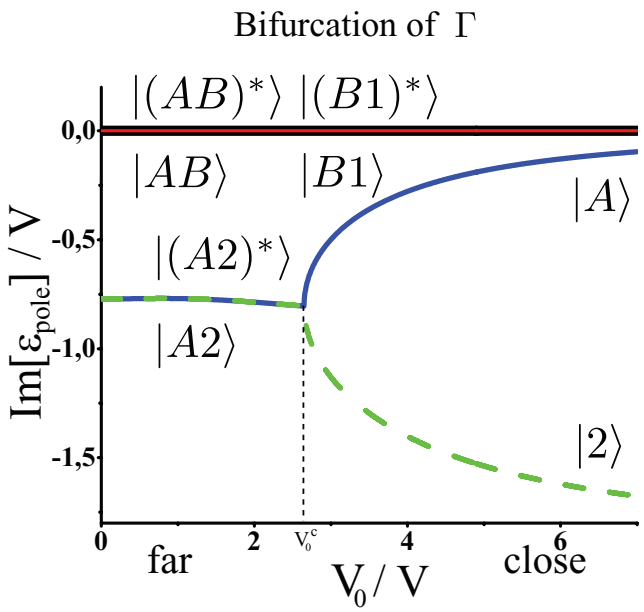

Figure 4. Bifurcation of decay rates. The imaginary part of the poles is plotted versus the V_0 molecule–substrate interaction. Small V_0 values represent a far away molecule. Black and red lines over the abscissa account for the infinite lifetime of the localized states out of the band. At V_0^C the imaginary part of the resonances (blue and green curves) show bifurcation. One branch accounts for a the increasingly long-lived atomic level, and the other branch describes the uncertainty of $|2\rangle$ that transforms it into the metallic delocalized band.

which for $V_0 = 0$ correspond to the bonding $(|A\rangle + |B\rangle)/\sqrt{2}$ (shorted as $|AB\rangle$) and antibonding $(|A\rangle - |B\rangle)/\sqrt{2}$ (shorted as $|(AB)^*\rangle$) localized states of the lonely molecule (i.e. H_2) at $\mp V_{AB}$. When V_0 increases strongly, e.g. for $V_0 = 3V$, these energies split further and become bonding and anti-bonding states between $|B\rangle$ and $|1\rangle$ orbitals, $|B1\rangle$ and $|(B1)^*\rangle$, respectively. As in the quantum Zeno effect, increasing this interaction would dissociate the A atom from the rest of the system [31]. This does not preclude a small amount of tunneling of A into the substrate's second layer passing through the orbitals B and 1. For intermediate V_0, this originates a through-bond interaction [23] that favors the formation of a bonding state between $|A\rangle$ and $|2\rangle$, as well as an antibonding one ($|A2\rangle$ and $|(A2)^*\rangle$, respectively). They are not localized states but resonances, because the electrons can be exchanged with the bulk.

The aforementioned resonances appear as poles of the Green's function with a finite imaginary part accounting for their coupling with the metal (figure 4). However, and this is the main point of this work, when V_0 increases and reaches V_0^C, a quantum phase transition occurs and the state $|A\rangle$ becomes almost purely atomic. Simultaneously, state $|2\rangle$ recovers its purely metallic nature. At the precise V_0^C of the transition the bonding and antibonding resonances (identified by the real parts of the poles) collapse into a degenerate value. Simultaneously, the pole's imaginary parts have non-analytic bifurcation into a decreasing part, which accounts for a long-lived atomic level, and an increasing uncertainty that represents the metallic delocalization of $|2\rangle$. This process can be interpreted as a manifestation of the Quantum Zeno Effect, meaning that when the interaction V_0 between atom B and the metal increases, the interaction between A and B becomes weaker [11, 31]. In addition, the imaginary part of the states out of the band remain zero for the whole range of V_0, due to the fact that they are localized states with an infinite lifetime.

At this point it is important to stress that the collapse of the real part of the poles at V_0^C occurs with an infinite slope, as in the experimental QDPT [11], a fact that is further clarified in figure 6. This indicates a first-order transition , such as the simple wide-band model discussed in the introduction. In a classical context, a first-order phase transition requires a total-energy level crossing for an infinite system. In the described molecule$\Longleftrightarrow$atomic quantum transition, a transition occurs at the level of resonances. A second-order character of the quantum phase transition, which would be associated with an acute crossing angle would be far more subtle, as it would involve singular quantum fluctuations. Although our mathematical approach can successfully account for diverging perturbation terms, no such acute angle was observed in the studied parametric regimes.

The detailed analysis of the spectral properties can be correlated with a study of the LDoS at different orbitals. Figure 5 shows the results from such an evaluation. In (a) and (b), we can see that for long distances ($V_0 \simeq 0$) the LDoS at $|A\rangle$ and $|B\rangle$ show a dominant presence outside the d-band. In contrast, (c) and (d) show that the sites 1 and 2 of the metal do not have appreciable participation at these energies. As the molecule approaches the surface and V_0 increases, the LDoS at the orbital $|A\rangle$, shown in figure 5 (a), loses its weight over the states outside the d-band. When $V_0 \approx V$, we observe the emergence of two broad resonances inside the band accounting for the $|A2\rangle$ and $|(A2)^*\rangle$ orbitals. Close to the non-analyticity point V_0^C, we observe that both resonances collapse into a single peak at $\varepsilon = E_A = 0$. This is precisely the energy of an electron at the isolated orbital $|A\rangle$.

An interesting complementary behaviour is observed on the LDoS at $|2\rangle$. Figure 5(d) shows that as V_0 increases, the two separate peaks, typical of a second layer [32], become close and almost collapse. They are still separated by anti-resonance [23], i.e. destructive interference with $|A\rangle$, which manifests as a pole for equation (9).

In figure 5 (c) we observe that as V_0 increases, the first metal site starts losing participation on the d-band. Simultaneously, it increases its participation on the bonding and antibonding states localized outside the d-band. Accordingly, the $|B\rangle$ orbital maintains substantial weight in these localized states (figure 5 (b)). This accounts for the fact that after the phase transition, when atom A decouples from B, the out-of-band localized states become the bonding and antibonding $|B1\rangle$ and $|(B1)^*\rangle$.

One might wonder how these prediction match with those of more realistic DFT calculations, such as the H_2 molecule interacting with a silver catalyst [4]. A first interesting effect, reproduced by DFT calculations and observed in the tight binding model, is the screening effect that the furthest atom suffers because of the presence of the adsorbed one. This result is observed in our LDoS on the bonding energies outside the

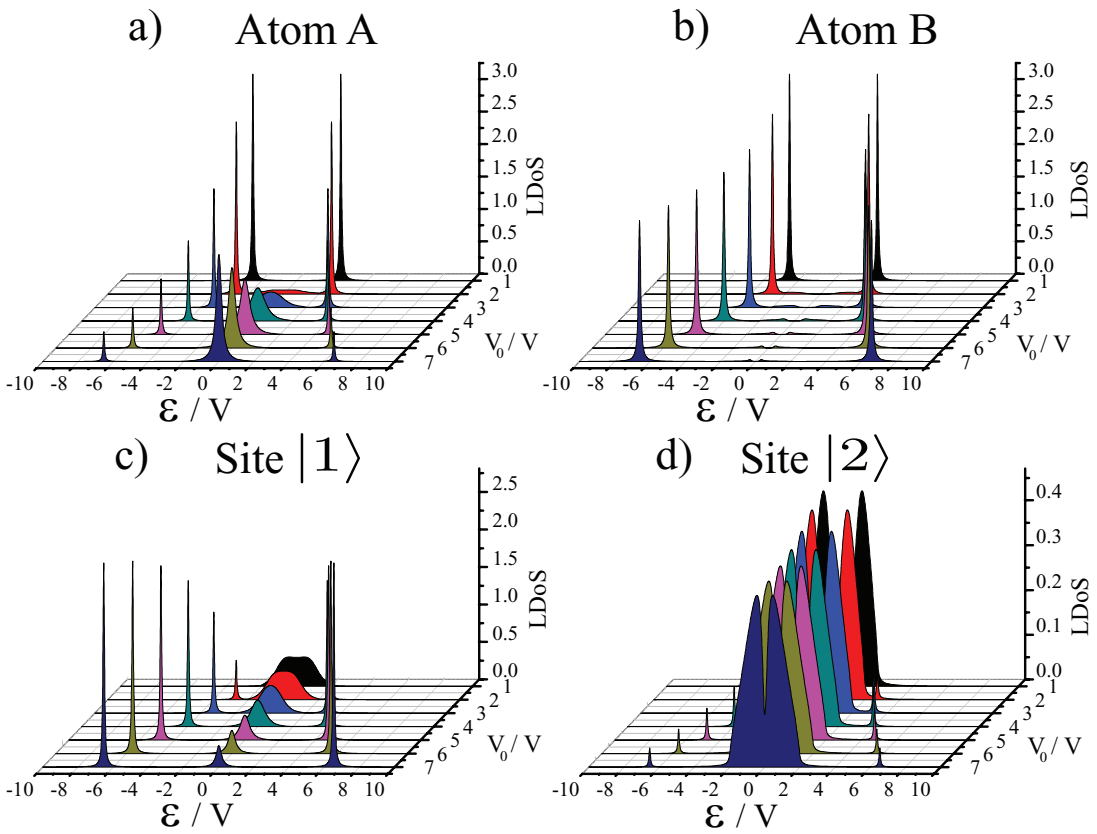

Figure 5. LDoS for different atoms and metallic sites. (a) and (b) A and B atomic orbitals, respectively. (c) and (d) 1 and 2 effective metal orbitals, respectively. For atom A we observe a decrease of the LDoS over the energies outside the band and an increment of its participation on the d -band resonances. Atom B, instead, does not lose its participation over the states outside the d-band as V_0 increases. The metallic orbital $|1\rangle$ loses its participation inside the band and gains presence over the localized states. The LDoS at orbital $|2\rangle$ shows almost no participation in the localized states outside the band. Consistently, the anti-resonance at the band centre ensures no mixing with $|A\rangle$.

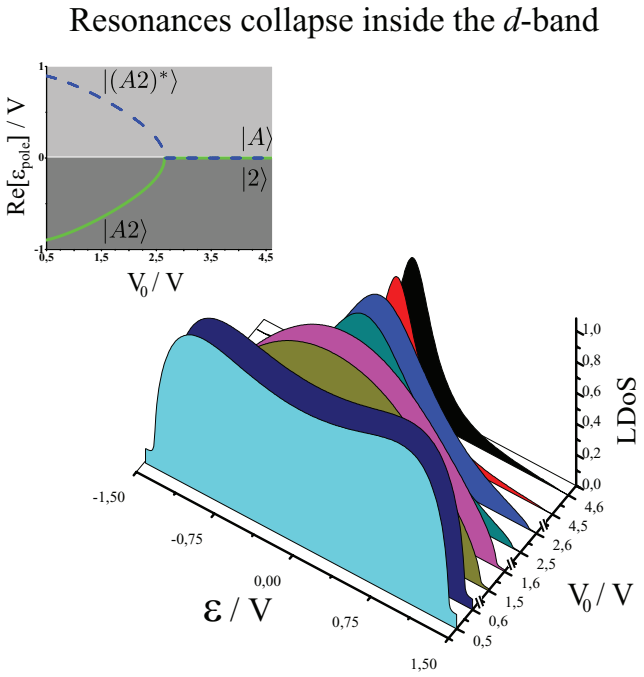

Figure 6. LDoS of A inside the d-band normalized to the local maximum. There we can see the two broad resonances collapse as V_0 reaches V_0^C. This collapse describes the Quantum Dynamical Phase Transition. Furthermore, after V_0^C the LDoS becomes narrower as A becomes isolated.

d-band of figure 5. There, the participation of the $|A\rangle$ orbital is smaller than that of $|B\rangle$. However, the highly structured d-band masks the spectral branching that characterizes a QDPT and is made evident in our tight-binding model after renormalization to the LDoS maximum (figure 6). Nevertheless, in DFT the hidden spectral bifurcation still constitutes the input for the full non-linear self-consistent calculation of the Coulomb interaction. Thus, it still may trigger the discontinuity on some of the observables that occur in the numerical solution. Although a hydrogen atom approaches another one adsorbed at the silver surface, a jump is observed in the total energy of the system. Simultaneously, the adsorbed atom also jumps to form the H_2 molecule. Thus, these discontinuities are consistent with the spectral discontinuities described by our QDPT model.

4. Conclusions

We analyzed the molecular dissociation in an Heterogeneous Catalysis process under the framework of Quantum Dynamical Phase Transitions [11, 18, 20]. As hinted by Anderson [29], the non-analyticity of the observables is an emergent phenomenon enabled by an infinite number of environmental degrees of freedom, in this case provided by the catalyst's d-band. We first observe a smooth crossover of the localized bonding and antibonding molecular states, which

lie outside the narrow *d*-band, into a bonding and antibonding combination between the closest atomic orbital and the first layers of the metal *d* orbitals. By reducing the LCAO model to a non-Hermitian Hamiltonian in which the imaginary parts have specific non-linear dependence on energy, we show that this system undergoes a collapse of resonances that provides the key to understanding the dissociation phenomenon. More specifically, each of the resonances is formed from the bonding and antibonding interaction between the furthest atom and a combination of *d* orbitals at the second layer of the metal. Before the molecule dissociation, both resonances are equivalently broadened by the rest of the metal. However, due to the interaction with the surface they merge into a collective metallic molecular orbital centered in the second layer of the substrate and an isolated atomic orbital at the center of the *d*-band.

In summary, we show that molecular dissociation constitutes a striking example of the Quantum Dynamical Phase Transition, a simple but non-trivial phenomenon that could emerge only because we dealt with the thermodynamic limit through non-Hermitian Hamiltonians.

Acknowledgments

We acknowledge financial support from CONICET (PIP 112-201001-00411), SeCyT-UNC, ANPCyT (PICT-2012-2324), and DFG (research network FOR1376). We thank P Serra and W Schmickler for discussions and references.

References

[1] Anderson P W 1972 More is different *Science* **177** 393–6
[2] Pastawski H M 2007 Revisiting the fermi golden rule: quantum dynamical phase transition as a paradigm shift *Physica B: Condensed Matter* **398** 278–86
[3] Heyrovsky J 1925 Researches with the dropping mercury cathode: part III. A theory *Recueil des Travaux Chimiques des Pays-Bas* **44** 499
[4] Santos E, Hindelang P, Quaino P and Schmickler W 2011 A model for the heyrovsky reaction as the second step in hydrogen evolution *Phys. Chem. Chem. Phys.* **13** 6992–7000
[5] Sachdev S 2007 *Quantum Phase Transitions* (New York: Wiley)
[6] Chibbaro S, Rondoni L and Vulpani A 2014 *Redutionism, Emergence and Levels of Reality* (Berlin: Springer)
[7] Anderson P W 1961 Localized magnetic states in metals *Phys. Rev.* **124** 41–53
[8] Newns D M 1969 Self-consistent model of hydrogen chemisorption *Phys. Rev.* **178** 1123–35
[9] Hoffmann R 1988 A chemical and theoretical way to look at bonding on surfaces *Rev. Mod. Phys.* **60** 601–28
[10] Majorana E 1932 Atomi orientati in campo magnetico variabile *Nuovo Cimento* **9** 43–50
[11] Álvarez G A, Danieli E P, Levstein P R and Pastawski H M 2006 Environmentally induced quantum dynamical phase transition in the spin swapping operation *J. Chem. Phys.* **124** 194507
[12] Gross M and Haroche S 1982 Superradiance: an essay on the theory of collective spontaneous emission *Phys. Rep.* **93** 301–96
[13] Celardo G L, Auerbach N, Izrailev F M and Zelevinsky V G 2011 Distribution of resonance widths and dynamics of continuum coupling *Phys. Rev. Lett.* **106** 042501
[14] Liu C, Di Falco A and Fratalocchi A 2014 Dicke phase transition with multiple superradiant states in quantum chaotic resonators *Phys. Rev.* X **4** 021048
[15] Hepp K and Lieb E H 1963 On the superradiant phase transition for molecules in a quantized radiation field: the dicke maser model *Ann. Phys. (N.Y.)* **76** 360
[16] Dicke R H 1954 Coherence in spontaneous radiation processes *Phys. Rev.* **93** 99–110
[17] Berry M B 2004 Physics of nonhermitian degeneracies *Czech. J. Phys.* **54** 1039–47
[18] Rotter I 2009 A non-hermitian hamilton operator and the physics of open quantum systems *J. Phys. A: Math. Theor.* **42** 153001
[19] Moiseyev N 2011 *Non-Hermitian Quantum Mechanics* (Cambridge: Cambridge University Press)
[20] Eleuch H and Rotter I Exceptional points, phase rigidity and nonlinear Schrödinger equation arXiv:1409.1149v1
[21] Dente A D, Bustos-Marún R A and Pastawski H M 2008 Dynamical regimes of a quantum swap gate beyond the fermi golden rule *Phys. Rev.* A **78** 062116
[22] Xin H, Vojvodic A, Voss J, Nørskov J K and Abild-Pedersen F 2014 *Phys. Rev.* B **89** 115114
[23] Levstein P R, Pastawski H M and D'Amato J L 1990 Tuning the through-bond interaction in a two-centre problem *J. Phys.: Condens. Matter* **2** 1781
[24] Haydock R, Heine V and Kelly M J 1972 Electronic structure based on the local atomic environment for tight-binding bands *J. Phys. C: Solid State Phys.* **5** 2845
[25] Santos E, Bartenschlager S and Schmickler W 2011 Electron transfer to heteronuclear diatomic molecules *J. Electroanal. Chem.* **660** 314–9
[26] Cattena C J, Bustos-Marún R A and Pastawski H M 2010 Crucial role of decoherence for electronic transport in molecular wires: polyaniline as a case study *Phys. Rev.* B **82** 144201
[27] Pastawski H M and Medina E 2001 'Tight binding' methods in quantum transport through molecules and small devices: from the coherent to the decoherent description *Rev. Mex. Fis.* **47** 1–23
[28] Cattena C J, Fernández-Alcázar L J, Bustos-Marún R A, Nozaki D and Pastawski H M 2014 Generalized multi-terminal decoherent transport: recursive algorithms and applications to saser and giant magnetoresistance *J. Phys.: Condens. Matter* **26** 345304
[29] Anderson P W 1978 Local moments and localized states *Rev. Mod. Phys.* **50** 191–201
[30] Fiori E R and Pastawski H M 2006 Non-markovian decay beyond the fermi golden rule: survival collapse of the polarization in spin chains *Chem. Phys. Lett.* **420** 35–41
[31] Facchi P and Pascazio S 2002 Quantum zeno subspaces *Phys. Rev. Lett.* **89** 080401
[32] Schrieffer J R and Soven P 2008 Theory of the electronic structure *Phys. Today* **28** 24–30